Electronic Supplementary Material (ESI) for Journal of Materials Chemistry C.
This journal is © The Royal Society of Chemistry 2019

Supplementary Information

Engineering carbon quantum dots for enhancing broadband photoresponse in silicon process line compatible photodetector

K. Sarkar[1], Pooja Devi[2], A. Lata[1], R. Ghosh[1] and Praveen Kumar[1]*

School of Materials Science, Indian Association for the Cultivation of Science, Kolkata 700032

Central Scientific Instruments Organization, Sector-30C, Chandigarh- India-160030, India

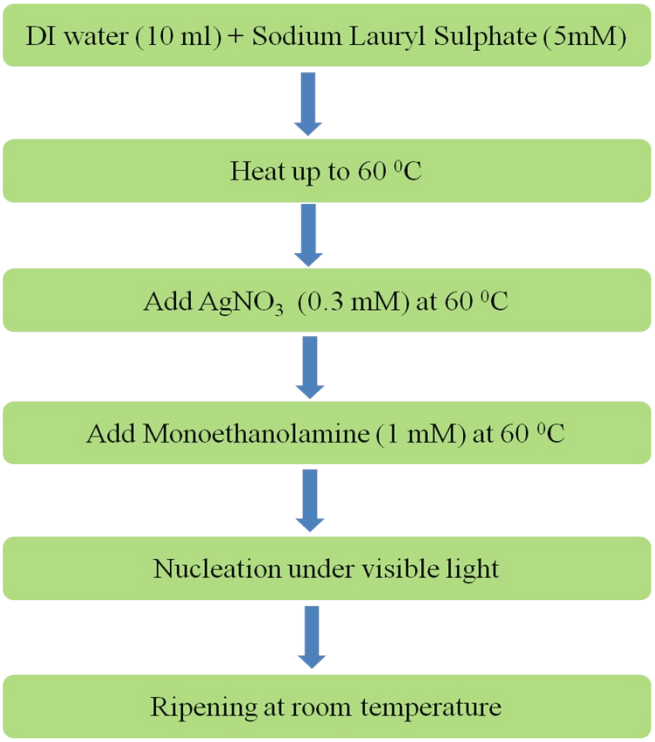

Figure S1. Process steps for synthesizing AgNPs

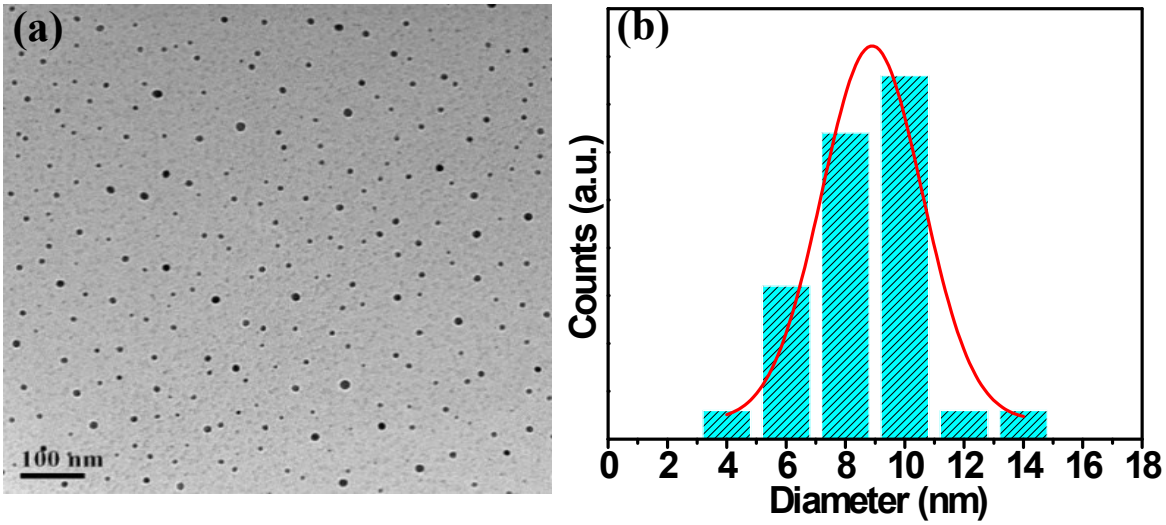

Figure S2. (a) Transmission electron microscope image of AgNPs. (b) Histogram showing size distribution with an average diameter at 9 nm.

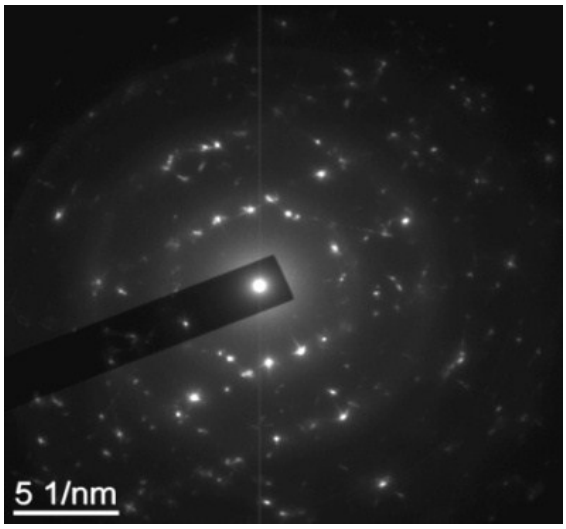

Figure S3. Selected area electron diffraction due to AgNPs reveals polycrystalline structure.

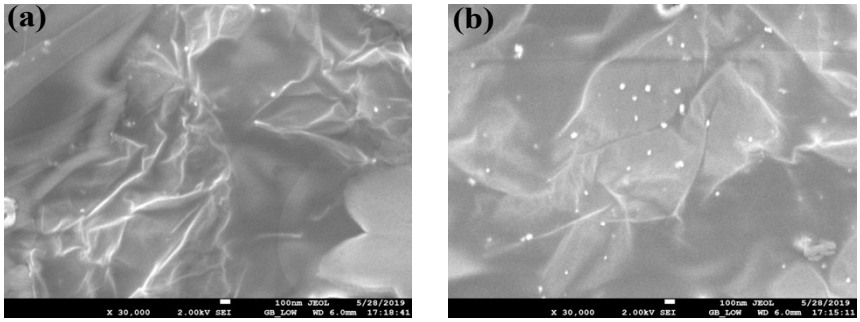

Figure S4. Scanning electron microscope image of (i) rGO-CQD composite, (ii) rGO-CQD-AgNP composite

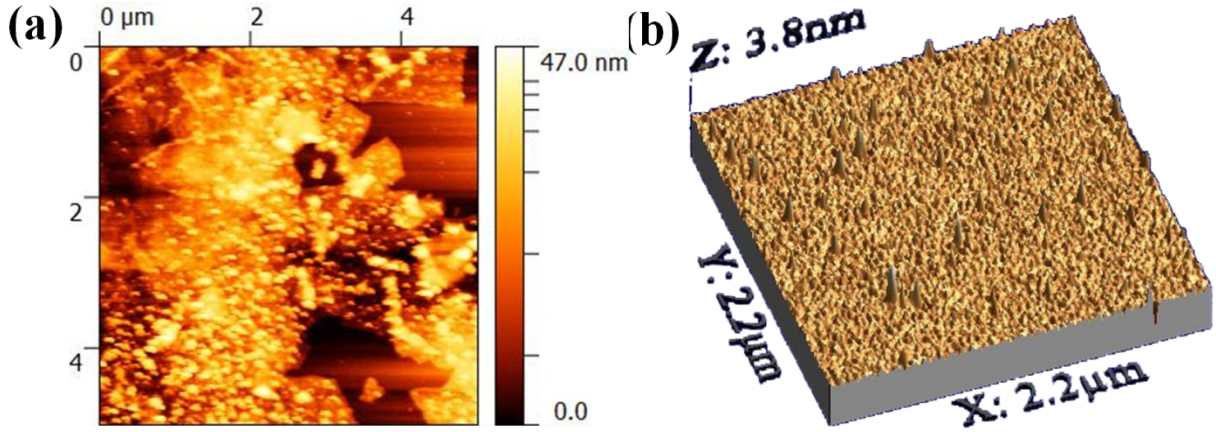

Figure S5. (a) Atomic force microscopy of S3 sample displays layers of rGO with randomly distributed nanostructures on it. (b) AFM image of CQDs coated on Si shows regular distribution over the scanned area.

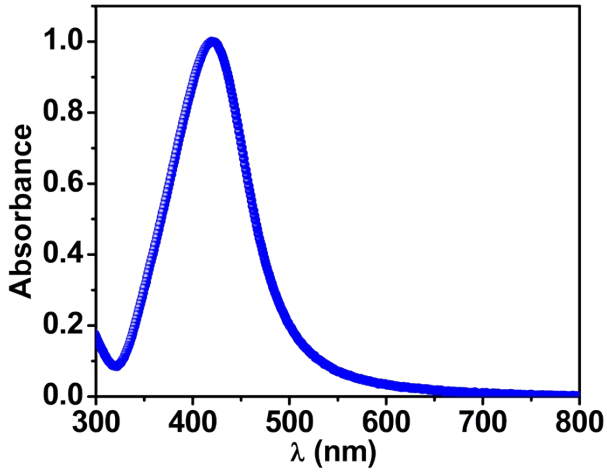

Figure S6. UV-Vis absorption spectroscopy of AgNPs displays localized surface plasmon resonance at 420 nm.

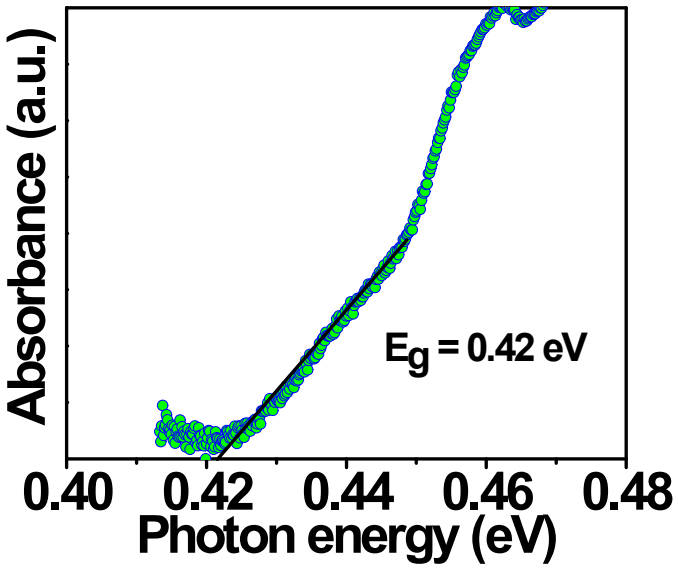

Figure S7: Optical bandgap of rGO estimated from absorption spectroscopy

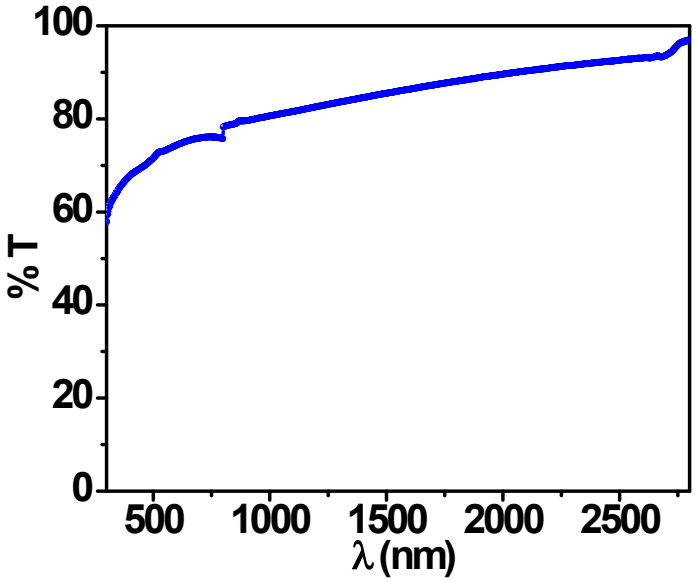

Figure S8: Broadband optical transmission from rGO (from UV to IR)

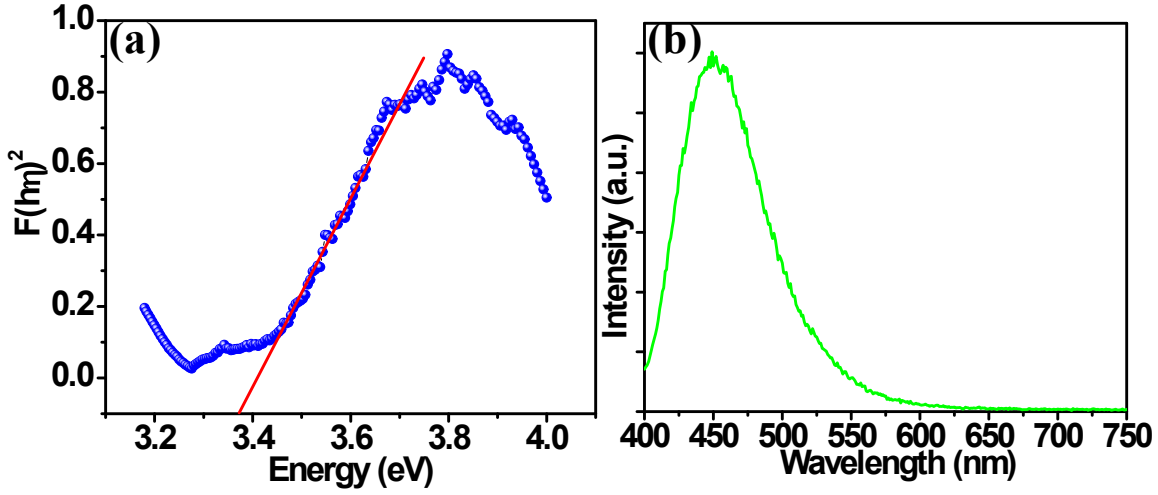

Figure S9. (a) Optical bandgap of CQD coated on Si substrate estimated by applying Kubelka-Munk theory. (b) Photoluminescence spectra of the CQDs exhibiting emission around 450 nm.

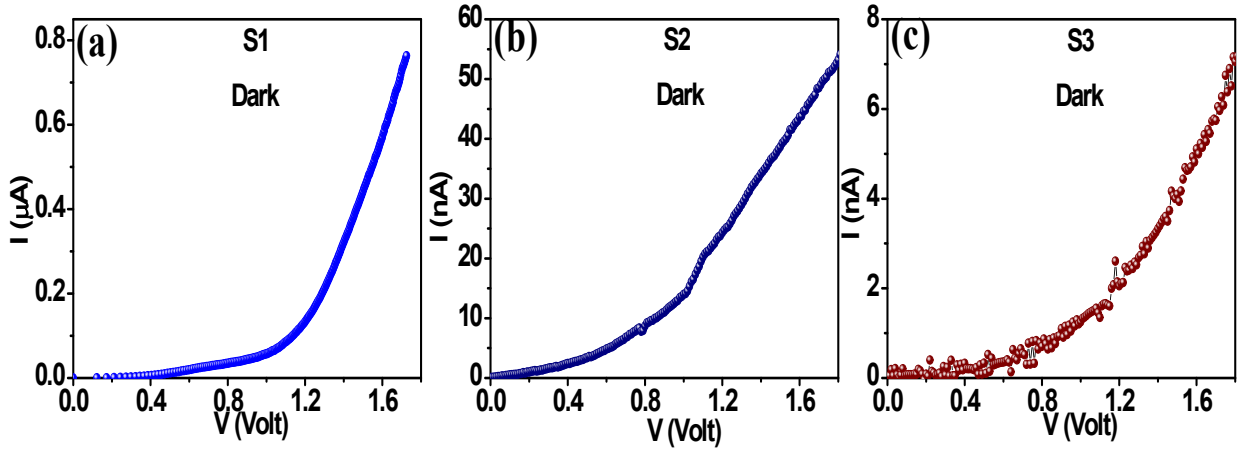

Figure S10. Dark current increases exponentially with a forward bias for all three sets of devices. S3 exhibits minimum dark current out of all sets of devices.

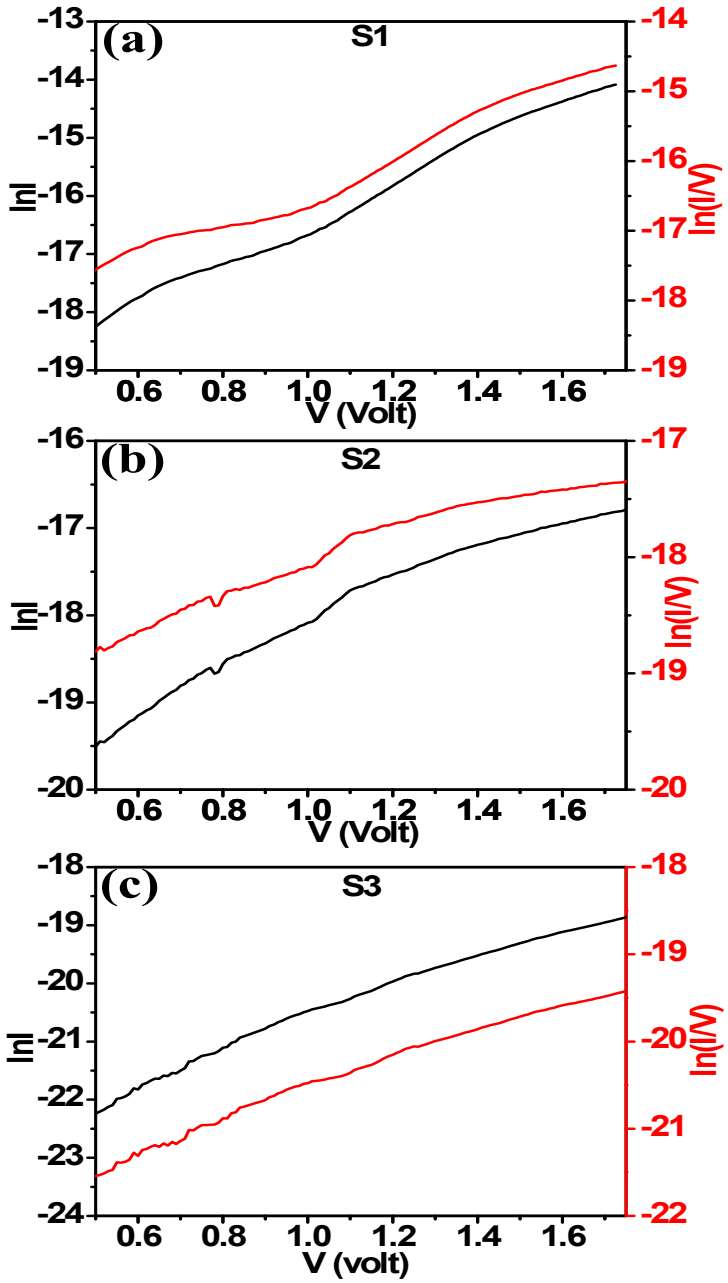

Figure S11: Semi-logarithmic plot of dark current with respect to forward bias voltage for three sets of devices. ln(I/V) as a function of forward bias for three sets of devices.

ESI Note: Figure S11 displays the variation of $ln\left(\frac{I}{V}\right)$ as a function of forward bias (V) for S1, S2 and S3 respectively in (a), (b) and (c). Sample S1 exhibits a continuously varying slope with increasing forward bias which signifies the gradual saturation of defect states and interfacial trap states through complex recombination process. In Sample S2 the distinct difference in the

variation of the slope is observed compared to S1 which can be ascribed to the diminished trap states due to reduced graphene oxide. Whereas in S3, almost constant slope is observed in $ln\left(\frac{I}{V}\right)$ vs V plot which signifies considerable decrease in unsaturated trap states due to highly reduced graphene oxide. Therefore, Sample S3 exhibits lowest value of ideality factor and highest value of on/off ratio under present experimental conditions.

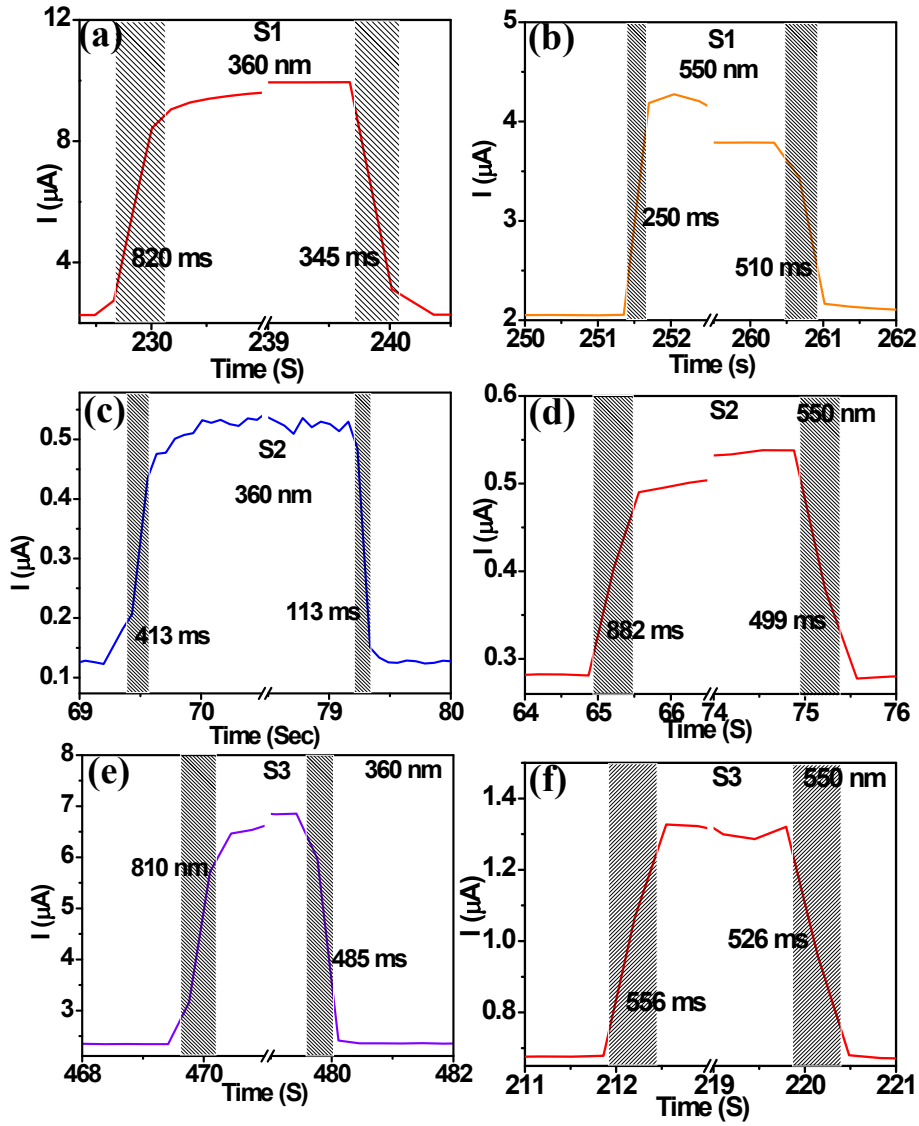

Figure S12. Calculation of rise time and fall time for three sets of samples under UV and Vis excitation.

Table T1: Estimated rise time and fall time

Sample	UV		Vis	
	t_r	t_f	t_r	t_f
S1	820 ms	345 ms	250 ms	500 ms
S2	413 ms	113 ms	882 ms	499 ms
S3	810 ms	485 ms	526 ms	562 ms

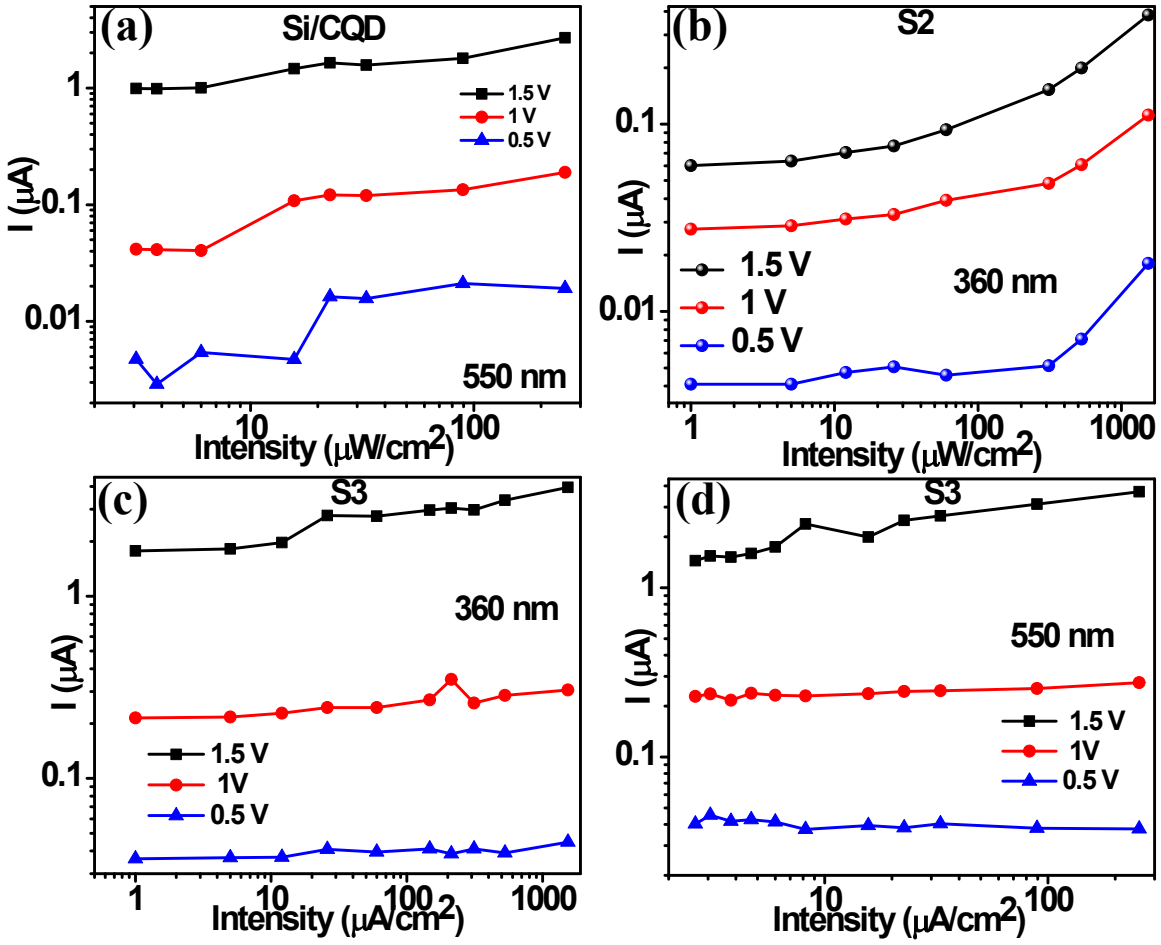

Figure S13. Photocurrent as a function of optical intensity

Table T2: Fitting parameters for excitation power dependence of three sets of devices

Sample	Fitting function	0.5 V			1 V			1.5 V		
		a	**b**	**c**	**a**	**b**	**c**	**a**	**b**	**c**
S1	$a + bx^c$	0.06	0.002	0.56	0.4	0.01	0.61	1.18	0.09	0.43
S2	$a + bx^c$	4.4×10^{-9}	10^{-13}	1.6	$3\times^{10-8}$	1.25×10^{-10}	0.88	6.2×10^{-8}	1.06×10^{-9}	0.78
S3	bx^c	--	0.03	0.04	--	0.2	0.06	--	1.49	0.13